AN ABSTRACT OF THE THESIS OF

Xin Huo for the degree of Master of Science in Genetics presented on January 5, 2006.

Title: Functional Analysis of the Pathogenic Mutation MLH1-E578G on Human MLH1 activity in DNA Mismatch Repair

Redacted for Privacy

Abstract approved: _____

Andrew B. Buermeyer

Mismatch repair (MMR) system performs mainly three roles to maintain genomic stability, correct DNA biosynthetic errors, ensure the fidelity of genetic recombination, and in mammalian cells participate in the cellular response to some DNA damages. Deficiencies in mismatch repair increase mutation rates and cancer risks. In eukaryotes, the MMR system contains several MSH (MutS homolog) and MLH (MutL homolog) proteins. Some germline mutations in human mismatch repair genes, mainly MSH2 and MLH1, have been found to be associated with Lynch Syndrome (as known as HNPCC, hereditary non-polyposis colorectal cancer). In this study, I examined the effect of a pathogenic mutation MLH1-E578G on MLH1-dependent error correction on base-base mismatch and dinucleotide loop. I conducted *in vitro* repair assay utilizing cell lines that express either wild-type or mutant MLH1 protein, and the 3'mismatched DNA substrates.

I successfully applied cytoplasmic extracts in *in vitro* repair assays, which might provide an easy way for studying other protein functions in human and mouse cell lines. By comparing the repair efficiency of base-base and dinucleotide loop DNA by both mutant and wild type MLH1, I found that the repair activity is dependent on MutLα concentration. In a 15-minute reaction, the mutant protein MLH1-E578G can support the repair of C-loop, CT-loop and G/T mismatch as well as wild-type MLH1. As suggested by the kinetics experiment, the in vitro MMR reactions are saturated at about 10 minutes; so a shorter time reaction time might be the best for *in vitro* repair comparisons. To have a better understanding of how MLH1-E578G contributes to an increased risk of disease, further studies need to be done.

Functional Analysis of the Pathogenic Mutation MLH1-E578G on Human MLH1 Activity in DNA Mismatch Repair

by

Xin Huo

A THESIS

submitted to

Oregon State University

in partial fulfillment of

the requirement for the

degree of

Master of Science

Presented on January 5, 2006

Commencement June 2006

Master of Science thesis of Xin Huo presented on January 5, 2006

APPROVED:

Redacted for Privacy

Major professor, representing Genetics Program

Redacted for Privacy

Head of the Genetics program

Redacted for Privacy

Dean of the Graduate School

I understand that my thesis will become part of the permanent collection of Oregon State University libraries. My signature below authorizes release of my thesis to any reader upon request.

Redacted for Privacy

Xin Huo, Author

ACKNOWLEDGEMENTS

Completion of this thesis would not have been possible without the support of mentors, colleagues, friends and family. First, I would like to thank my graduate committee for all of their support during the process. Dr. Andrew Buermeyer, my major professor from Environmental and Molecular Toxicology, was always available when I had questions regarding research. He gave me invaluable feedbacks when needed and supported me with different research options and ideas, and challenged me to write the thesis more clearly. I am grateful to Dr. Chris Mathews, Dr. William Baird and Dr. Michael Schimerlik from Biochemistry and Biophysics for their careful reading of the thesis and the insights they brought to my work.

I would also like to thank Dr. Huixian Wang and Dr. John Hays from Department of Environmental and Molecular Toxicology for providing me HeLa nuclear extracts and mismatched substrate for test of the system; and Dr. Michael Liskay from Oregon Health Science University for offering me the purified human MutLα.

Without question that I would express my gratitude to the great people from Andrew Buermeyer laboratory, Azizah Mohd, Bryan Ing, Eddie O'Donnell, Stephanie Smith-Roe, Karen Hippchen, Brett Palama, Jason Steindler and Scott Nelson, they provided me both assistance in research and friendship in life, and created a harmonious working environment in the

laboratory. I really enjoyed knowing them. Without all of them, I would have found the graduate years more painful.

I don't have words to adequately express my gratitude to my friends Ting Wu and Jing Wu for their love and friendship throughout my graduate study as in all other parts of my life, I will always be grateful to them.

Thanks to all the great friends I have met here at Oregon State University, they are too many to list here, but I will remember them forever.

Finally, I would also like to take this opportunity to thank my dear mom, dad and all family members for their unconditional love, support and encouragement in my life. Without them, I could not be where I am today.

TABLE OF CONTENTS

Page

CHAPTER 1. INTRODUCTION 1

1.1 BRIEF INTRODUCTION TO DNA MISMATCH REPAIR 1

1.2 MECHANISM OF MMR 2

1.3 MMR AND LYNCH SYNDROME 6

CHAPTER 2. MATERIALS AND METHODS 11

2.1 GENERATION OF MISMATCH-CONTAINING SUBSTRATES 11

2.2 CELL LINES 12

2.3 CYTOPLASMIC EXTRACT PREPARATION 13

2.4 WHOLE CELL LYSATE PREPARATION 13

2.5 MISMATCH REPAIR REACTIONS 13

2.6 PROTEIN EXPRESSION AND QUANTIFICATION 15

CHAPTER 3 EXPERIMENTAL RESULTS 16

3.1 OVERVIEW OF THE EXPERIMENTAL SYSTEM 16

3.2 SUBSTRATE DESCRIPTION AND PREPARATION 16

3.3 PRELIMINARY REPAIR REACTIONS WITH A G/T MISMATCHED SUBSTRATE 27

3.4 WESTERN BLOT ANALYSIS OF CYTOPLASMIC EXTRACTS 29

3.4.1 MMR in extracts of cells expressing different levels of MLH1 36

3.4.2 MMR in diluted cytoplasmic extracts 38

3.5 KINETICS OF MMR IN CYTOPLASMIC EXTRACTS 41

3.6 ACTIVITY OF MLH1-E578G IN MMR 45

CHAPTER 4. DISCUSSION 53

BIBLIOGRAPHY 58

LIST OF FIGURES

Figure Page

FIGURE 1 MISMATCH CORRECTION PATHWAY AND SCHEMATIC REPRESENTATION OF HUMAN MLH1 PROTEIN: 8
FIGURE 2 (A) SCHEMATIC OF REPAIR ASSAY (B) DNA MISMATCHED SUBSTRATES USED FOR THE REPAIR REACTIONS. 17
FIGURE 3 (A). PREPARATIONS AND PURIFICATION OF MISMATCHED DNA SUBSTRATES; (B) PUC19PA PLASMID MAP 19
FIGURE 4. GENERATION AND QUALITY CONTROLS OF GAP DNA 22
FIGURE 5. QUALITY TEST OF THE MISMATCHED DNA SUBSTRATES 25
FIGURE 6. NICKED PRODUCTS OF C-LOOP AND CT-LOOP BY N.BPU10I. 26
FIGURE 7. CORRECTION OF G/T MISMATCHED SUBSTRATES 30
FIGURE 8. WESTERN BLOT ANALYSIS OF MMR PROTEIN LEVELS IN CYTOPLASMIC EXTRACTS 32
FIGURE 9. MMR PROTEIN ABUNDANCE IN HELA NUCLEAR AND MEF CYTOPLASMIC EXTRACTS 33
FIGURE 10. MUTLα CONCENTRATIONS IN DIFFERENT EXTRACTS 35
FIGURE 11. MLH1 CONCENTRATION IN CYTOPLASMIC AND NUCLEAR EXTRACTS 37
FIGURE 12. REPAIR OF C-LOOP SUBSTRATE BY DIFFERENT WILD-TYPE MLH1 EXPRESSING CYTOPLASMIC EXTRACTS 39
FIGURE 13. REPAIR OF CT-LOOP SUBSTRATE BY DIFFERENT WILD-TYPE MLH1 EXPRESSING CYTOPLASMIC EXTRACTS 40
FIGURE 14. MMR PROTEIN LEVELS IN DILUTED CYTOPLASMIC EXTRACTS 42
FIGURE 15. REPAIR OF C-LOOP BY DILUTED WT-1 CYTOPLASMIC EXTRACT 43
FIGURE 16. REPAIR OF C-LOOP BY DILUTED WT-2 CYTOPLASMIC EXTRACT 44
FIGURE 17. KINETICS OF MMR IN CYTOPLASMIC EXTRACTS 47
FIGURE 18. STANDARD CURVE OF C-LOOP (A) AND CT-LOOP (B) REPAIR 50
FIGURE 19. C-LOOP MMR IN MLH1-E578G CYTOPLASMIC EXTRACTS 51

FIGURE 20 CT -LOOP MMR IN MLH1-E578G CYTOPLASMIC EXTRACTS..... 52

CHAPTER 1. INTRODUCTION

1.1 Brief introduction to DNA Mismatch Repair

DNA mismatch repair (MMR) is an evolutionarily conserved repair pathway that has an important role in protection against cancer development. Primarily, DNA mismatch repair (MMR) is responsible for the recognition and repair of base-base mismatches and insertion-deletion loops (IDL) generated during DNA replication (Kunkel, 2005). MMR activity contributes up to 1000 fold to the fidelity of DNA replication and thus helps keep the mutation rate at a low level (Harfe 2000, Modrich 1996). During recombination, MMR proteins can detect base-base mispairing in recombination intermediates and block illegitimate recombination events between divergent sequences in the genome. This function of MMR helps prevent deleterious genome rearrangements mediated by dispersed repetitive elements (Myung, Chen, Kolodner, 2001). In addition, MMR has been implicated in cellular functions apart from repair of mismatches. That provides an alternative means of protecting the genome. MMR proteins also recognize various base modifications caused by genotoxins, such as 8-oxo-guanine lesions caused by oxidative stress and O^6-methyl guanine caused by alkylating agents. MMR helps prevent mutations and is involved in the activation of cell cycle checkpoint pathways and signaling to apoptosis in response to such DNA damage (Bellacosa, 2001; Borts *et al*, 2000; Harfe and Jinks-Robertson, 2000; Junop *et al.*, 2003;

Kolodner and Marsischky, 1999, Li, 2003). The relative importance of the various functions of MMR in suppressing cancer risk is unknown.

1.2 Mechanism of MMR

The basic mechanism of DNA mismatch repair involves recognition of DNA mispairs (base-base or IDLs mismatches), excision of a patch containing the mismatch, re-synthesis and ligation (Schofield, 2003). This basic mechanism and the core protein components of MMR are conserved in prokaryotes and eukaryotes (Harfe, 2000).

In prokaryotes, represented by *E. coli*, a protein complex composed of two MutS proteins recognizes and binds to mismatches in post-replicative DNA. A homodimer composed of two MutL protein subunits, thought to act as a molecular matchmaker between the MutS-DNA complex and downstream factors, interacts with the MutS:DNA complex in an ATP-dependent manner, forming a ternary complex. MutL then activates the endonuclease MutH (Ban, 1998, Bocker, 1999), which nicks the newly synthesized and transiently unmethylated strand, at the closest GATC site located up to 1kb from the mismatch (Au, 1992, Hall, 1999). DNA helicase II and single strand binding protein, working together with one of several possible exonucleases, excise the mismatch-containing DNA strand, allowing replicating polymerase III to synthesize a corrected version (Modrich, 1991, 1996). The prokaryotic mismatch repair system has been reconstituted *in*

vitro using purified proteins and a synthetic plasmid substrate containing a single mismatch and one unmethylated strand (Lahue, 1989; Modrich, 1996; Schofield, 2003).

The MMR system in eukaryotes is more complex (Figure 1A). It includes multiple MutS homologs (MSH) and multiple MutL homologs (MLH), with the active forms being heterodimers composed of two different MSH or MLH proteins (Kolodner and Marsischky, 1999). The MutS homologs (MSH2, MSH3 and MSH6) form the heterodimers MSH2–MSH6 (MutSα) and MSH2–MSH3 (MutSß). MutSα recognizes base-base and small IDL mismatches, whereas MutSß recognizes both small and larger IDLs containing up to 16 extra nucleotides (Marsischky, 1996, Das Gupta 2000, Maculloch 2003). Thus there is some functional redundancy between MutSα and MutSß. Among MutL homologues, three heterodimers are known. MLH1/PMS2 (MutLα), MLH1/PMS1 (MutLß) and MLH1/MLH3 (MutLγ) (Li and Modrich, 1995; Lipkin *et al.*, 2000; Raschle *et al.*, 1999). MutLα plays the major role in MMR in partnership with MutSα and MutSβ, while the heterodimers MutLß and MutLγ play minor or redundant roles in mismatch repair. To date no convincing MutH homolog has been identified, so the origin or entry points for excision *in vivo* and the mechanism by which the MMR system distinguishes the newly synthesized strand from the template DNA are still not known. In biochemical reactions *in vitro*, a nick can direct excision to the nick-

containing strand, suggesting that the 3' terminus of the nascent DNA, or the 5' terminus of Okazaki fragments might serve as the excision origin.

Biochemical and genetic approaches have identified several additional proteins as necessary or implicated in MMR, including: PCNA (proliferating cell nuclear antigen) (Umar, 1996; Bowers, 2001), EXOI (exonuclease I), RPA (replication protein A) (Lin *et al,* 1998), RFC (replication factor C) (Genschel, 2003), HMG1 (high mobility group1) (Yuan, 2004), MRE11 (meiotic recombination) (Her, 2002). Among these, EXOI and MRE11 both have 3'-5' exonuclease activity, while EXOI also has 5'-3' activity; RPA is a single-strand DNA binding protein that could protect the single strand DNA during repair; RFC binds to the sliding clamp PCNA and helps load it onto DNA. In addition, Modrich and colleagues have developed a reconstituted human MMR system containing MutSα, MutLα, EXOI, RPA, PCNA, RFC and DNA polymerase δ. This system can support 5' directed MMR, albeit with a low efficiency (Schofield, 2003). However, despite extensive research efforts, the mechanism by which mismatch recognition is coupled to site-specific initiation of excision in eukaryotes or prokaryotes remains controversial. Currently there are three models to explain this coupling: the sliding clamp model, the ATP hydrolysis-dependent translocation model, and the induced fit model. In the first two models, mismatches bound in the presence of ATP by MSH heterodimers are coupled with MLH heterodimers to form ternary recognition complexes that move away along the DNA contour and search for excision-initiation signals—either by

ATP-hydrolysis-dependent translocation (Allen *et al*, 1997) or by ATP-binding-dependent diffusional sliding, with hydrolysis occurring later (Gradia *et al*, 1997, 1999; Wang, 2004). With ATP-hydrolysis-dependent translocation, a single motor protein complex is needed, whereas with the ATP-hydrolysis-independent sliding clamp model, multiple sliding clamps of MutSα heterodimers are needed (Fishel, 2001). Alternatively, with the induced fit model, MutS recognizes a heteroduplex DNA and remains at the mismatch, rather than moving along the DNA, searching is accomplished through space for excision-initiation signals, facilitated by DNA bending (Junop *et al*, 2001; Schofield *et al*, 2001; Wang, 2004). In this model, MutL is proposed to stabilize the ternary complex.

The MLH1 protein consists of three domains (Figure 1B), the amino terminal domain (approximately amino acids 1-350), the linker domain (residues 350-500), and the carboxyl-terminal PMS2/EXOI interaction domain (amino acids 500-756). The main function of amino terminal domain is ATP binding and hydrolysis, ATP binding results in conformational changes leading to dimerization of the N-termini (Tomer, 2002). The amino terminal domain also contains a subdomain for ssDNA binding, formed when the N-termini associate (Hall 2003). ATP binding and hydrolysis, N-terminal heterodimerization and ssDNA all appear necessary for MMR; however, precise roles remain uncharacterized. The C-terminal domain is necessary for adenosine nucleotide-independent heterodimer interaction, and for interactions with EXOI interaction. It has been shown that the interactions are

important for recognition of nuclear localization sequences in MLH1 and PMS2. This domain has also been shown to be necessary for promoting the stability of PMS2 (Mohd, 2005).

1.3 MMR and Lynch Syndrome

Colorectal cancer is the third most deadly type of cancer in US society. Inherited germline mutations in the DNA mismatch repair (MMR) genes MSH2 or MLH1 can result in Lynch Syndrome (also known as hereditary non-polyposis colorectal cancer or HNPCC), an autosomal-dominant cancer syndrome characterized by early-onset colorectal and other internal cancers. Depending on the population and clinical criteria used, Lynch Syndrome may comprise 2–8% of all colorectal cancers, making it the most common inherited predisposition cancer syndrome. Lynch Syndrome cancers often are identified by the presence of microsatellite instability (MSI), an elevated frequency of mutation in microsatellites (short, repeated sequences) throughout the genome. However, some cancers that fit the Lynch Syndrome profile have low levels or no apparent MSI (Raevaara *et al,* 2005) and some cancers have high levels of MSI but a defect in MMR proteins has not been detected. Although mutations in PMS2 and MSH6 have been observed, the majority (approximately 90%) of the MMR gene mutations identified in Lynch syndrome patients are in MSH2 or MLH1 (Peltomaki, 2001). Germline genetic testing of individuals suspected of Lynch

syndrome has revealed over 330 different alterations in MLH1 genes. Approximately one-third of the MLH1 alterations identified in human cancers are single amino acid substitutions whose functional consequence is not immediately obvious. These 'variants of uncertain significance' require further investigation to determine whether each may be a pathogenic mutation or a silent polymorphism.

A main focus of work in our laboratory is to determine whether mutations in MLH1 found in human cancers are likely to be pathogenic mutations by measuring the effect of such mutations on different functions of MLH1. This study is focused on a specific MLH1 mutation, MLH1-E578G that was identified as a germline mutation in several suspected Lynch Syndrome patients. Several tumors in patients with the MLH1-E578G variant were MSI-negative, prompting interest in this mutant (Liu 1999). This residue maps to the loosely defined PMS2 interaction domain. However, the pathogenicity of this mutation has been controversial: Guerrette *et al.* (1999) reported that MLH1-E578G showed a 54% reduction in binding to PMS2. Study in yeast using the dominant mutator effect of human MLH1 cDNA found this mutant to be pathogenic (Shimodaira, 1999), while another yeast study using two-hybrid (Kondo, 2003) assay showed human MLH1-E578G binds to human PMS2 as well as wild-type human MLH1. In preliminary studies, our laboratory compared the ability of MLH1-E578G and wild-type MLH1 to complement the MMR-deficiency of mouse embryonic fibroblast (MEF) cells

A.

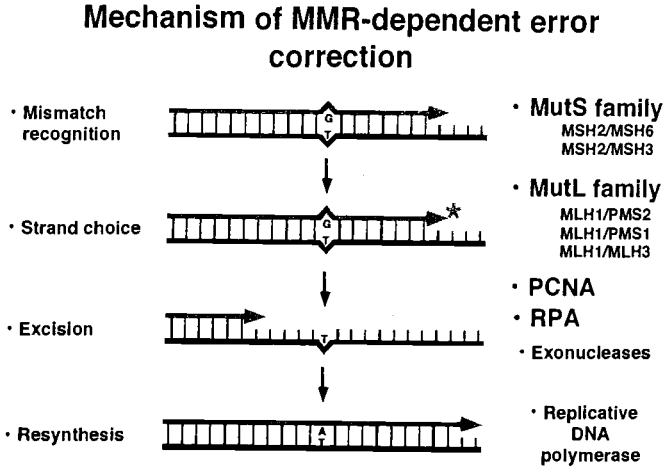

B.

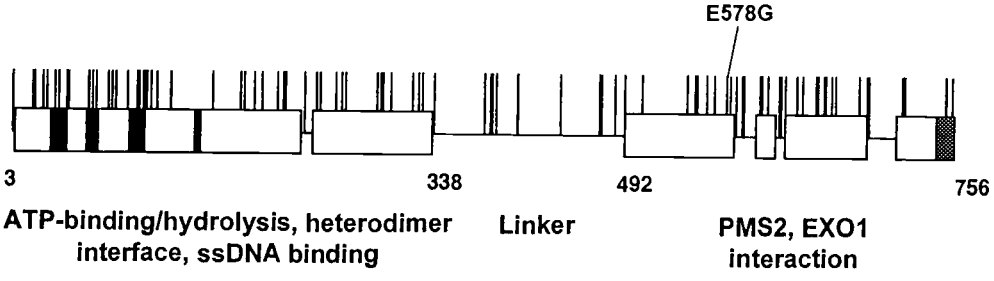

FIGURE 1 MISMATCH CORRECTION PATHWAY AND SCHEMATIC REPRESENTATION OF HUMAN MLH1 PROTEIN:

(A) Depicts the error correction function of MMR and proteins involved in the process, details provided in the text. (B) Depicts approximate boundaries of different domains of MLH1 including: the ATP binding domain, PMS2 and EXOI interaction domain, the linker domain, and the location of MLH1-E578G. White boxes represent the sequences conserved in human and yeast MLH1; black bars the

sequences necessary for ATP binding and hydrolysis, whereas vertical lines indicate the location of pathogenic mutations listed in the Human Gene Mutation Database (http://www.hgmd.cf.ac.uk/hgmd0.html).

lacking MLH1. Similar to wild-type MLH1, stable expression of MLH1-E578G reduced the frequency of microsatellite mutations and increased the cytotoxic responses to the DNA damaging drug 6-Thioguanine. However, the rate of base substitutions remained elevated in cells expressing MLH1-E578G. Thus, the E578G mutation might affect specifically the ability of MLH1 to function in repair of base-base mismatches. An elevated base substitution mutation rate could partially explain an increased cancer risk associated with MLH1-E578G.

To test the hypothesis that MLH1-E578G is capable of repairing IDLs while being defective in base-base mismatch correction, I conducted *in vitro* MMR assays using cytoplasmic extracts of cells expressing wild-type MLH1 or MLH1-E578G and circular DNA substrates containing either a base-base mismatch or a dinucleotide loop mismatch. I established that MMR-competent extracts could be generated routinely from MEFs stably-expressing MLH1 and determined that repair activity in such extracts is linearly dependent upon MLH1 concentration. Thus MLH1 appears to be a limiting factor for repair in such extracts, suggesting the *in vitro* system is an appropriate model for the analysis of functional consequences of MLH1 mutations. In addition, in findings inconsistent with my hypothesis, this assay provided preliminary evidence that MLH1-E578G is capable of repairing both base-base and IDL mismatch-containing substrates.

CHAPTER 2. MATERIALS AND METHODS

2.1 Generation of Mismatch-containing Substrates

Plasmid substrates containing site-specific mismatches and a single nick were generated and purified as described (Wang and Hays, 2001). Briefly, pUC19PA (Figure 3) was digested with endonuclease N.AlwI or N.Bst.NBI, and the 30-nt oligomers between the resulting nicks were removed by heating to 85°C and cooling to room temperature over approximately 3 hours in the presence of 50-fold excess of oligomer complementary to the displaced 30-mer. Single strand and double stranded oligomers in the mixture were separated from plasmid DNA by centrifugation through a Centricon-100 filter (Milipore) with 4 washes of TE buffer. Gapped plasmids were purified by benzoylated-naphoylated-DEAE cellulose (BND-cellulose) chromatography as described. Gapped DNA was incubated for 10 minutes at room temperature with 30 ml of BND cellulose resin slurry in TE buffer containing 1 M NaCl, with shaking. The mixture was poured into a 50-ml disposable polypropylene column yielding a settled bed volume of approximately 10 ml. The column was washed with 100 ml TE buffer containing 1.0 M NaCl, and eluted with 20 ml CFS buffer (2% caffeine, 50% formamide, 1.0 M NaCl, 10 mM Tris-HCl, pH8.0, 1 mM EDTA). Fractions (1 ml) were collected and analyzed by agarose gel electrophoresis; appropriate fractions were pooled, dialyzed against TE buffer 4 times at 4°C and concentrated to approximately 200 μl by centricon-100 filtration. To generate the C-loop and CT-loop mismatched

substrates, 5'-phosphorylated oligomers **TCTATGCGCACGTTAACATGGAGAGTCGCTC** or **ACGTAAGCTTCGAGGTGAATAGGATCATCG** were ligated into either the N.Bst.NBI-gapped or N.AlwI-gapped plasmids respectively. The gap molecules and oligos were incubated in 1x ligation buffer at 50°C for 5 minutes, and then allowed to cool to room temperature, fresh ATP (0.5 mM) and T4 ligase (1unit/200 ng DNA) were added for overnight ligation at 16°C. The ligated products were purified from the nicked by centrifugation through a cesium chloride gradient (Sambrook and Russell 2001), dialyzed 4 times against one liter of 1x TE each time, and concentrated by centricon-100 filtration. N.Bpu10I was used to introduce a single nick in the plasmid substrate, and dialysis and concentration were repeated to yield the final substrate preparation. It is important to store the final substrate in a buffering system instead of water. After several freezing-thaw cycles, the closed circle mismatched plasmid stored in water shows a significant amount of random nicking (data not shown).

2.2 Cell lines

HeLaS3 cells (gift of H. Wang and J. Hays, Oregon State University), an MMR-proficient human cancer cell line, were used as a source for nuclear extracts that served as a positive control for the *in vitro* repair assays. WT-1, WT-2, WT-3, WT-4 and WT-5 are MLH1-deficient MEF cell lines stably transfected with wild-

type MLH1 cDNA (Buermeyer 1999), whereas vector-1, 2 cells were transfected with a plasmid without the MLH1 cDNA. The cell line MLH1-E578G-1 was generated in a similar manner to express the mutant MLH1-E578G (Buermeyer, unpublished)

2.3 Cytoplasmic Extract Preparation

Cytoplasmic extracts were prepared as described (Tomer, Buermeyer *et al*, 2002). Briefly, approximately $1x10^8$ cells were harvested with trypsin, swelled on ice with hypotonic buffer (20 mM HEPES, pH7.9, 5 mM KCl, 1.5 mM $MgCl_2$, 1 mM dithiothreitol, 0.1 mM phenylmethylsulfonyl fluoride) (0.7 ml/10^8 cells), and lysed with 20 strokes of a tight fitting pestle and dounce. After incubation on ice for 30 minutes, the lysate was clarified by centrifugation. The supernatant was aliquoted to 50 μl each, snap frozen in liquid nitrogen, and stored at –80°C.

2.4 Whole Cell Lysate Preparation

Trypsinized cells were collected by centrifugation (1000x g), rinsed twice with 1x PBS, re-suspended with 5 packed cell volumes of cold PBS, and lysed with a similar volume of 2x lysis buffer [100 mM Tris-Cl pH 6.8; 4% (w/v) SDS; 20% (v/v) glycerol, 200 mM DTT]. The mixture was boiled for 5 minutes and stored at –80°C.

2.5 Mismatch Repair Reactions

MMR reaction mixtures (15 μl) contained 75 fmole of c-loop, CT-loop, or 23 fmole of G/T mismatched substrate, 100 μg of cytoplasmic extract protein, and 750 ng of bovine serum albumin, plus the following components at the indicated concentrations: 20 mM Tris-HCl, pH 7.6; 4 mM ATP; 1 mM glutathione; 0.1 mM for each of four dNTPs; 5 mM $MgCl_2$; and 110 mM KCl. Mixtures were incubated at 37 °C for 15 min unless otherwise indicated. Reactions were terminated by the addition of 30 μl of Stop solution (25 mM EDTA, 0.67 % SDS, and 90 μg/ml proteinase K). After further incubation at 37 °C for 15 min, DNA was extracted twice with an equal volume of phenol and precipitated with ethanol. DNA was resuspended in H_2O and digested with 5 units of FspI (C-loop) or XhoI + PvuI (CT-loop), HindIII + ClaI (G/T mismatch) endonucleases and 1 μg of RNase A at 37 °C for 2 h in 10 μl of digestion buffer (50 mM Tris-HCl, pH 7.9; 100 mM NaCl; 10 mM $MgCl_2$; and 1 mM DTT). The digested products were separated by electrophoresis in 1% agarose gel using 1x TAE buffer (40 mM Tris acetate, 2 mM EDTA). Correction of the CT-loop mismatch restores the site for XhoI endonuclease (Figure 2B and 3), yielding 0.7 kb and 1.4 kb fragments following an XhoI, PvuI double digest. Correction of the C-loop mismatch generates a second FspI (Figure 2B) site in the plasmid, yielding 0.7 kb and 1.4 kb following digestion with FspI. DNA bands were visualized by staining with ethidium bromide, imaged using a Kodak Image Station 440. Band intensities were determined using Kodak 1D analysis software (Molecular Imaging and Cell Culture Core, Environmental

Health Science Center, Oregon State University). The repair percentage was calculated as the ratio of the summed intensities representing repaired bands to the total of this sum plus the intensity of the band corresponding to singly cut (nonrepaired) DNA.

2.6 Protein expression and quantification

Protein expression in different cell lines was compared by western blot analysis of whole cell lysates. The concentration of specific MMR proteins in cytoplasmic or nuclear extracts was determined similarly. All protein samples were electrophoresed on 4-12% Criterion Gels (Bio-Rad) at 200v for 55 minutes, followed by transfer to PVDF membrane using a Bio-Rad wet transfer apparatus 100v for 30 minutes. Following transfer, the membrane was blocked with 5% blotto [w/v of powder milk in 1x TBST (53.3 g NaCl, 1.3 g Kcl, 20 g Tris-base, 100 ml tween in 10 Liter H_2O)] for at least 1 hour at room temperature, and incubated at room temperature using the indicated dilutions of commercially available antibodies: anti-human MLH1, (BD Pharmingen, clone G168-728; 1:1000), PMS2 (BD Pharmingen, clone GA16-4; 1:1000) and MSH6 (BD Pharmingen, clone 44; 1:2500). The secondary antibody GAM-IgG-HRP conjugate (1:10000) (Pierce) was incubated for 1 hour with shaking. Chemiluminescence signal was detected using the Kodak Image Station 440 followed by quantification using Kodak 1D analysis software.

CHAPTER 3 EXPERIMENTAL RESULTS

3.1 Overview of the experimental system

To determine the effect of the potentially pathogenic mutation MLH1-E578G on MLH1-dependent error correction of base-base mismatches and dinucleotide loops, I performed *in vitro* MMR assays utilizing cytoplasmic extracts (Thomas *et al,* 1995) of cell lines that express either wild-type or mutant human MLH1 protein, and the DNA substrates containing a single defined mismatch and nick. With this assay, cytoplasmic extracts and the mismatched DNA substrate are combined together, and incubated at 37°C in the presence of ATP, $MgCl_2$, and dNTPs. Excision is initiated from the pre-existing nick and proceeds towards the mismatch, terminating at 150 bases past the mismatch. DNA resynthesis and ligation follow, completing the repair reaction and restoring a unique restriction endonuclease site. The repaired product is then screened by diagnostic restriction endonuclease digestion (Figure 2A).

3.2 Substrate description and preparation

PUC19PA, with two tandem N.Bst.NBI or N.AlwI endonuclease recognition sites separated by 30 bases on the same strand (Figure 3B), was manipulated step by step as described (Wang & Hays, 2001) to generate the final mismatched substrates. Details of the procedure are described in Materials and

A.

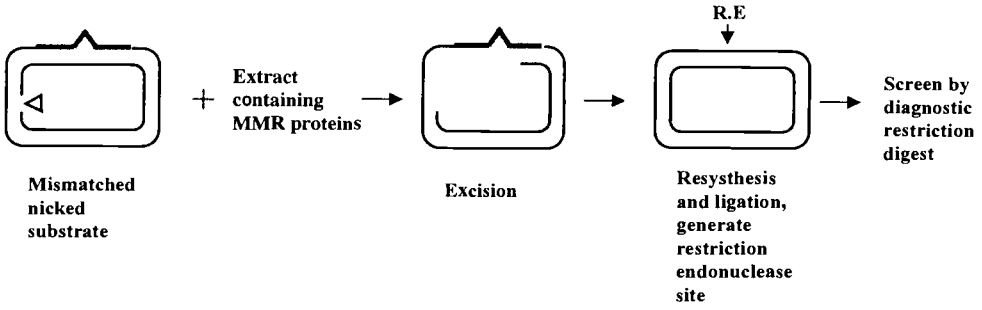

B.

C-loop

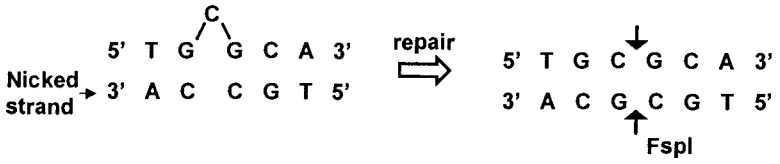

CT-loop

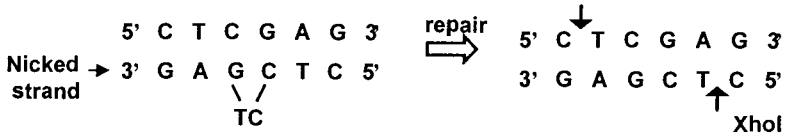

G/T mismatch

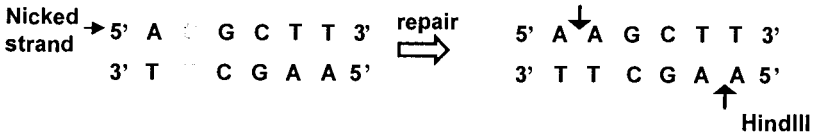

FIGURE 2 (A) SCHEMATIC OF REPAIR ASSAY (B) DNA MISMATCHED SUBSTRATES USED FOR THE REPAIR REACTIONS.

A. Details of the repair assay provided in Materials and Methods. B. The C-loop, CT-loop and G/T mismatched substrates and the restriction sites generated after repair are shown.

Methods (section 2.1). Treatment with nicking endonuclease yields doubly nicked DNA and some incompletely digested singly nicked DNA. Partial denaturation and reannealing in the presence of a large excess of 30 mer complementary to the putative incision product yields gapped DNA. Purification of gapped molecules is accomplished by filtration (to remove oligos) and BND cellulose chromatography. BND cellulose chromatography is important for the separation of gapped molecules from the nicked contaminants. Generally the singly nicked DNA is not retained by BND cellulose whereas the gapped DNA is retained due to binding of the single-stranded gap to the column matrix. Specific mismatches then are generated within gaps by ligating appropriate 5'-phosphorylated oligos, followed by isolation of ligated plasmids by CsCl high-speed centrifugation.

The pUC19PA plasmid DNA was obtained by use of a Qiagen anion-exchange plasmid mega kit and further purified by centrifugation through a CsCl gradient. CsCl-banding generally is necessary to limit random DNA nicks, especially for DNA purified from an *E. coli* strain lacking Dam methylase. However, CsCl banding generally yields preparations with approximately 5% nicked plasmid and is not necessary if the Qiagen DNA preparation already has less than 5% nicked plasmid. To generate mismatched plasmid substrates, 800 μg of pUC19PA plasmid DNA was treated with the nicking enzymes N.Bst.NBI (for preparation of a C-loop mismatch) or N.AlwI (for a CT-loop mismatch), partially denatured in the presence of an excess of complementary oligo, and purified by

A

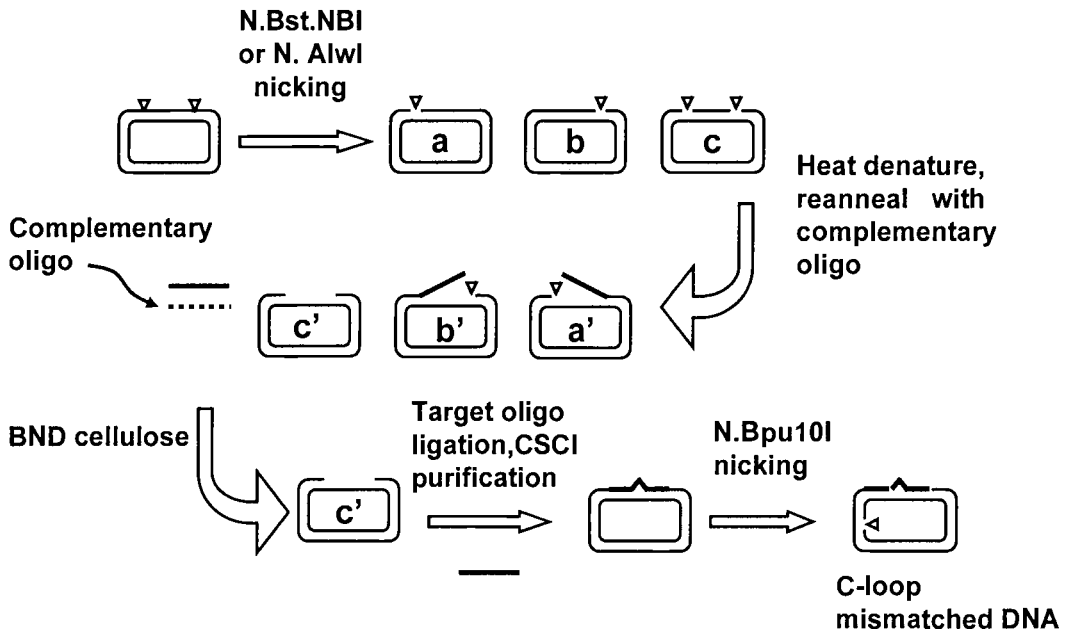

B

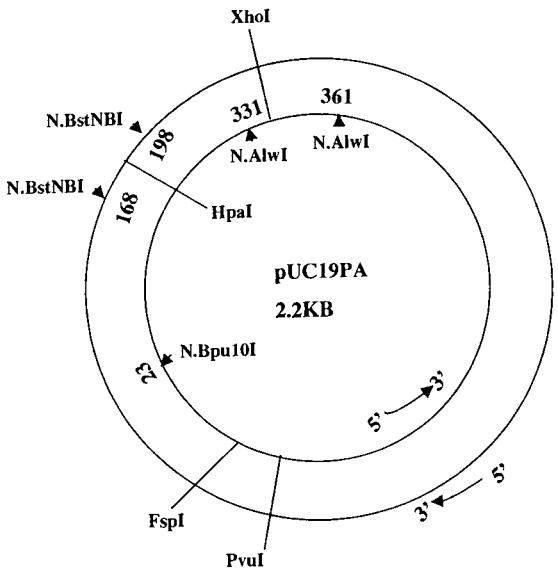

FIGURE 3 (A). PREPARATIONS AND PURIFICATION OF MISMATCHED DNA SUBSTRATES; (B) PUC19PA PLASMID MAP

(B) PUC19PA contains N.Bst.NBI sites at position 168 and 198, and N.AlwI sites at position 331 and 361, used to generate the C-loop or CT-loop mismatched substrates respectively. A site at position 23 for the nicking endonuclease N.Bpu10I, was used to generate a single nick 3' to the mismatch for the initiation of excision and repair. Positions of the XhoI (position 339), Hpa I (position 182) and PvuI (position 1769) sites used for diagnostic digestions are indicated on the map.

using BND-cellulose chromatography (Figure 3A). Plasmid DNA recovered following BND-cellulose was analyzed by restriction digestion and analytical agarose gel electrophoresis. Gap generation using N.Bst.NBI affects an HpaI site in pUC19PA (Figure 3B), so the gapped molecule would be resistant to HpaI digestion. Similarly, the XhoI site in the original plasmid is affected by gap generation using N. AlwI. In contrast, non-gapped contaminating plasmid in the gapped DNA preparation should be sensitive to digestion with either HpaI or XhoI. As expected, N.Bst.NBI and N. AlwI gapped DNA co-migrated with open circle (nicked) plasmid, and generally was resistant to digestion with HpaI or XhoI, respectively (Figure 4), suggesting that appropriately gapped plasmids were generated and purified. Although linearized DNA was detected in the N.AlwI-gapped DNA preparation, it appeared to be less than 5% of the total, and this was concluded to be an acceptable level of contamination.

Starting with 800 μg of plasmid DNA pUC19PA, approximately 300 μg of N.Bst.NBI gapped and 150 μg of N. AlwI gapped plasmid were obtained after BND cellulose chromatography.

To generate closed circle plasmids containing a site-specific C-loop or CT-loop mismatch, 5'-phosphorylated oligomers

5' -TCTATGCGCACGTTAACATGGAGAGTCGCTC-3' or

A

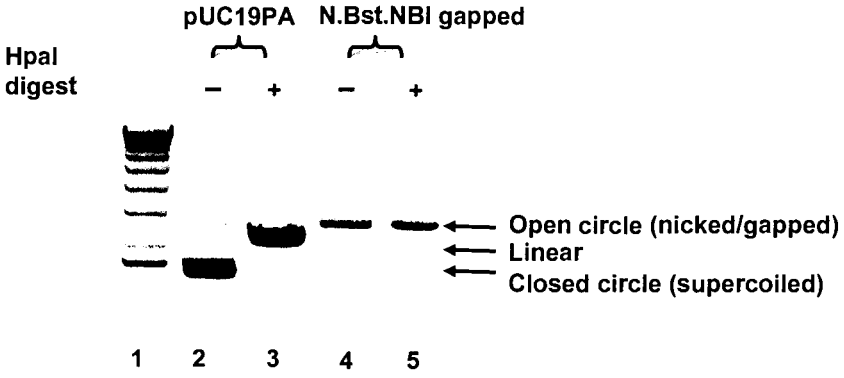

B

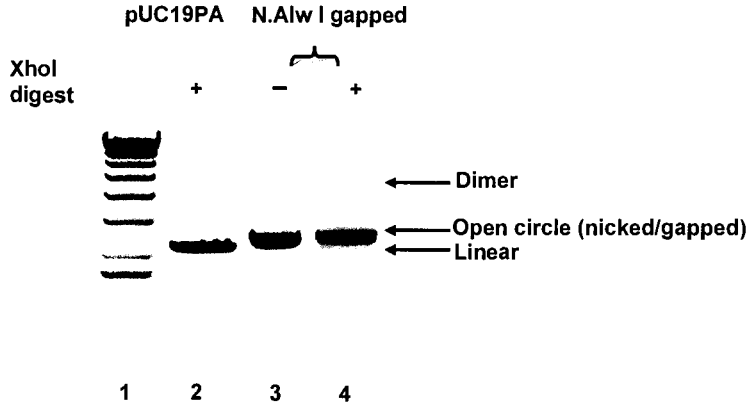

FIGURE 4. GENERATION AND QUALITY CONTROLS OF GAP DNA

Gapped DNA was generated as described in Materials and Methods; and the quality of the preparation was tested by restriction digestion. (A) HpaI digest on C-loop gap, pUC19PA as closed circle control and HpaI digested pUC19PA included to indicate migration of linearized plasmid; (B) XhoI digest on CT-loop gap, XhoI digested pUC19PA as linear control.

5'- ACGTAAGCCTCCTGAGGTGAATAGGATCATCG - 3' were annealed and ligated into single stranded gaps created by N.Bst.NBI or N.AlwI, respectively. Test ligations under different conditions, varying temperature, incubation times and 5'-phosphorylated oligonucleotides from different manufacturers, were performed (data not shown), and the ligation conditions that yielded the highest efficiency were used. C-loop oligo ligation yielded approximately 50% of closed circle product, and CT-loop oligo yielded approximately 65% efficiency (data not shown). Closed circle plasmid was purified by high-speed centrifugation through CsCl gradients.

To demonstrate that purified plasmids indeed contained the desired mismatch, closed circle plasmid DNA was incubated with FspI (for C-loop) or XhoI (for CT-loop). As shown in Figure 5A, the C-loop plasmid was resistant to cleavage by Fspl. In contrast, approximately 25% of the CT-loop plasmid preparation was sensitive to XhoI. The XhoI and PvuI double digest yielded 3 bands, 2.1 kb, 1.4 kb and 0.7 kb (not shown), indicating that the CT-loop plasmid contained contaminating plasmid DNA lacking the desired mismatch. The contaminating DNA likely was the starting plasmid pUC19PA that co-purified through BND cellulose as a nicked plasmid. When complementary oligos were added during generation of the gapped molecule (Figure 3A), the complementary oligos could bind stably to a "flap" formed by partial denaturation of singly nicked plasmid. Such "flapped" homoduplex molecules could be retained on the BND-

cellulose matrix due to single-stranded DNA exposed by the flap, subsequently eluting with gapped plasmids. To remove the contaminating homoduplex plasmid, an XhoI digest was used to linearize the contaminating DNA followed by digestion with RecBCD (Epicentre), a bi-directional exonuclease that specifically degrades the linear fragment and not nicked or gapped plasmids. Following treatment with RecBCD, the plasmid was religated to seal any nicks, and re-purified by CsCl gradient centrifugation. The supercoiled plasmid (Figure 5B, lane 5) was again tested for sensitivity to XhoI digestion (Figure 5B, lane 6); the presence of one linear band confirms that the final CT-loop mismatched DNA is in good quality (i.e. digested with PvuI, but resistant to XhoI). Analysis of the XhoI/PvuI restriction digest demonstrated that more than 95% of the purified DNA now was resistant to XhoI (Figure 5B lanes 5, 6), indicating the presence of the desired CT-loop mismatch. Final yields of the closed circle mismatched plasmids were 20 μg for the CT-loop and 70 μg for the C-loop mismatches.

In the last steps of the substrate preparation, a single site-specific nick was introduced in both the C-loop and CT-loop mismatched plasmids using the commercially available nicking enzyme N. Bpu10I (Figure 6). N.Bpu10I nicks the C-loop DNA 150 bps 3' to the mismatch whereas in the CT-loop plasmid, the nicking site is 300 bps 3' of the mismatch (Figure 2B). N. Bpu10I nicked 100% of the supercoiled C-loop and CT-loop DNA, as indicated by the shift in migration (Figure 6 lanes 4, 5).

A

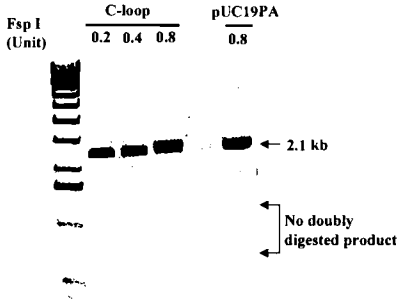

B

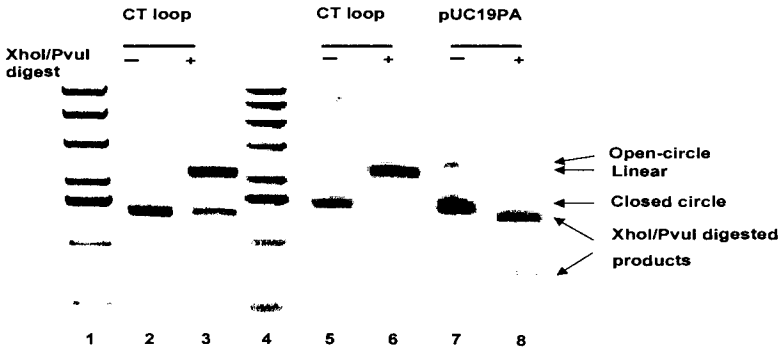

FIGURE 5. QUALITY TEST OF THE MISMATCHED DNA SUBSTRATES

The quality of C-loop and CT-loop mismatched plasmids was assured by restriction digest. (A) Shown is the C-loop plasmid digested with FspI. Resistance to digestion indicates the presence of the desired mismatch.100 ng of C-loop substrate or pUC19PA plasmid DNA was incubated with indicated units of Fsp1. (B) Quality of final CT-loop mismatched plasmid. Shown is the CT-loop mismatched plasmid and the XhoI/PvuI double digestion before (lanes 2, 3) and after (lanes 5, 6) RecBCD purification. Linearization with PvuI was used to allow detection of XhoI-sensitive plasmid more easily. The untreated pUC19PA plasmid (lane 7) and digested with XhoI/PvuI (lane 8) are included as migration controls.

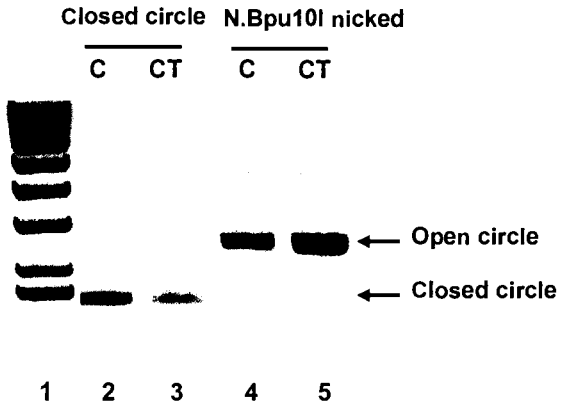

FIGURE 6. NICKED PRODUCTS OF C-LOOP AND CT-LOOP BY N.BPU10I.

Closed circle mismatched C-loop or CT-loop DNA (lanes 2, 3) were nicked by incubation with N.Bpu10I, and dialyzed for buffer exchange (lanes 4, 5).

3.3 Preliminary repair reactions with a G/T mismatched substrate

As a source of MMR factors including MLH1, cytoplasmic extracts (Thomas *et al,* 1991) were prepared from various derivative cell lines of either MLH1-deficient mouse embryonic fibroblasts (MEFs) (Buermeyer, 1999) or a human MLH1-deficient ovarian cancer cell line (MNU-1). Derivative cell lines were generated by transfection and selection with G418-sulfate to isolate clones stably expressing MLH1 (hereafter WT-1 through WT-6) or the variant MLH1-E578G (E578G-1, 2), or with stably integrated plasmid lacking MLH1 cDNA (Vector-1, 2). Cell lines were generated and characterized for cellular phenotypes by others in the Buermeyer laboratory (Steindler, Mohd and Buermeyer, unpublished). The validity of the "cell complementation" approach is supported by demonstration that stable expression of a human MLH1 cDNA can restore MMR in MLH1-deficient MEFs (Buermeyer 1999), which also highlights the high degree of conservation of the mammalian MMR system.

Previous studies of MMR *in vitro* have utilized either nuclear (Holmes, 1990; Wang, 2003) or cytoplasmic extracts (Tomer, 2002), and generally results have been consistent with the two systems. One advantage of the cytoplasmic extract system is that extracts can be prepared from fewer cells (approximately 10^8) than with nuclear extracts (generally 10^9-10^{10} cells), which greatly facilitates preparations from adherent cell lines. A second advantage is that MMR-active

cytoplasmic extracts have been prepared previously from MEFs (Tomer, 2002), although in those experiments, recombinant MutLα purified after expression in insect cells was used. In vitro repair using transfected MEF cell lines stably expressing human MLH1 has not been reported. In addition, repair in cytoplasmic extracts initiated from both 5' and 3'-nicks requires MutLα, whereas in nuclear extracts, only 3'-nick directed repair is MutLα dependent (Genschel, 2002). The molecular basis for this difference is not known.

To determine if the cytoplasmic extract MMR system would work using transfected MEF lines, I conducted in vitro repair reactions using a G/T mismatched DNA substrate (kindly provided by Wang/Hays, OSU) and cytoplasmic extracts of a MEF cell line expressing either wild-type human MLH1 or the variant MLH1-E578G (Figure 7). Previous western blot analysis of whole cell lysate (Mohd, Steindler and Buermeyer, unpublished) indicated that the WT-4 and E578G-1 cell lines expressed similar levels of MLH1. Repair reactions included 100 μg extract, 100 ng substrates (23 fmoles) and 15' incubation. HeLa nuclear extract is a well-established source of MMR proteins in the literature (Thomas *et al,* 1991, Wang, 2000, 2003), and was included as a positive control; with this G/T mismatched plasmid, repair yield was approximately 60% of input substrate in a 15-minute reaction with HeLa nuclear extract (Figure 7). With cytoplasmic extract of wild-type MLH1 expressing MEFs (WT-4), repair yield was 38%. Similar repair yield was seen with cytoplasmic extracts of MLH1-E578G

expressing MEFs (E578G-1). As expected, extracts of cells transfected with the empty vector and reactions without added extract did not yield any repaired products. Homoduplex DNA was included in the restriction digest analysis of repair products to provide a migration marker for plasmid cleaved by HindIII. Thus, the overall approach using transfected cells expressing MLH1 should work. In addition, the results suggested the MLH1-E578G variant was proficient in repair of G/T mismatches, and that HeLa nuclear extract was more active than cytoplasmic extracts of MEFs. However, it was unknown whether the tested conditions were appropriate for a quantitative comparison. In particular, the concentration of MLH1 (MutLα) in the various extracts was not known. Also, whether MutLα was in excess or whether repair yields had saturated within 15 minutes were not known. Therefore, to establish conditions appropriate for a quantitative comparison of the activity of wild type versus variant MLH1, The *in vitro* repair system was characterized further using cytoplasmic lysates of transfected MEFs. The following sections of this thesis describe quantitation of MutLα in cytoplasmic extracts, the dependence of repair yield on MLH1 concentration, and the kinetics of the appearance of repaired products.

3.4 Western blot analysis of cytoplasmic extracts

From various available cell lines that expressed MLH1, MLH1-E578 or that were transfected with empty vector, cytoplasmic extracts were prepared and the

A

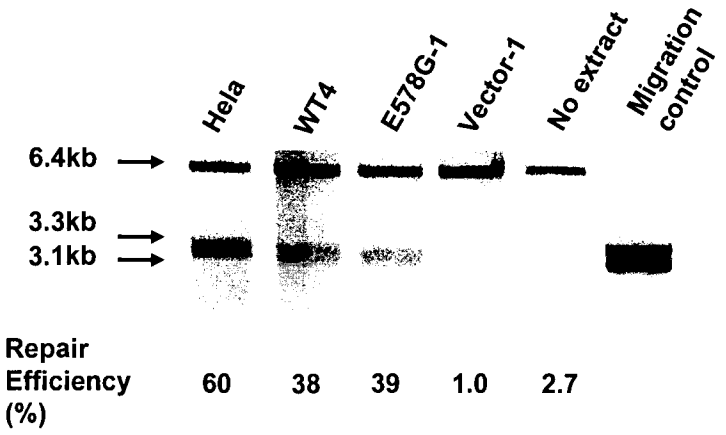

FIGURE 7. CORRECTION OF G/T MISMATCHED SUBSTRATES

Repair reactions included 100 μg of HeLa nuclear extracts or cytoplasmic extracts of transfected MEFs, 100 ng of 3' nicked G/T mismatched substrate. Repair was scored following a 15-minute incubation and digestion of the recovered plasmids with HindIII and ClaI. The arrows indicate unrepaired DNA (6.4 kb band) and repaired DNA (3.3 and 3.1 kb bands). Fractions of the input substrate repaired (cleaved by the indicated endonucleases) were calculated by quantitative imaging of the bands. Data correspond to one representative experiment of 3 with similar results.

relative levels of MLH1, PMS2 and MSH6 (Figure 8) were determined by western blot analysis. MLH1 was detectable at similar levels in 2 transfectants examined. WT-1 and WT-2, with lower expression in the WT-4 cell line, indicating variation among different transfected cell lines. As expected, no MLH1 signal was detected in extracts of the vector-1 transfectant that received the control vector, and in extracts of an MMR-proficient MEF cell line MC-5, as the antibody used does not recognize the endogenous mouse MLH1. MLH1 level in the MLH1-E578G transfected cell line (E578G-1) (lane 9, 10) was similar to WT-4, but lower than WT-1 and WT-2. High levels of MLH1-E578G also were not detected in several other transfectants (data not shown). Also as expected, PMS2 protein levels were reduced in extracts of vector-transfected cells compared to MLH1-expressing cells, (lane 7, 8 versus lane 1-6), consistent with the previous reports that the presence of MLH1 protects PMS2 from degradation in cells (Buermeyer 1999, Mohd 2005).

MMR protein abundance in cytoplasmic extracts also was compared to the abundance in HeLa nuclear extracts (Figure 9). While MSH6 levels were comparable in both types of extracts, MLH1 and PMS2 were significantly more abundant in the nuclear extract. In contrast, a comparison of the whole cell lysate of HeLa cells and transfected MEFs suggested that MLH1 and PMS2 are concentrated in nuclei, consistent with their apparent nuclear localization as determined by immunohistochemical analysis (Mohd 2005).

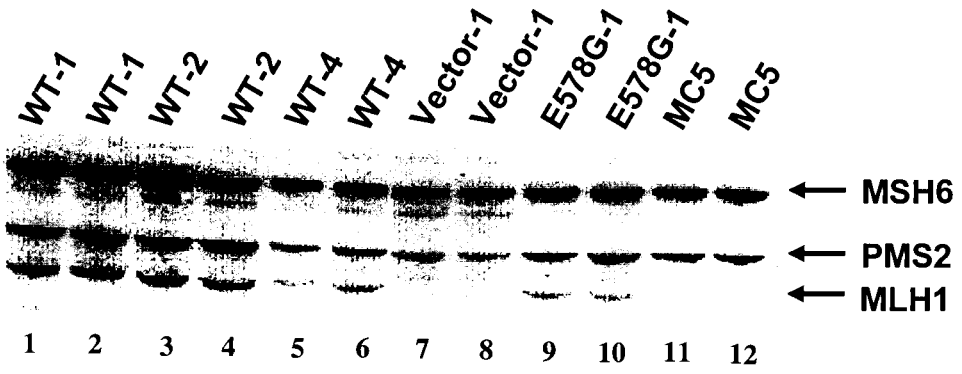

FIGURE 8. WESTERN BLOT ANALYSIS OF MMR PROTEIN LEVELS IN CYTOPLASMIC EXTRACTS

Approximately 30 μg of total cytoplasmic extracts protein were separated on a 4-12% SDS polyacrylamide gel, transferred and probed with anti-human MLH1, anti-mouse PMS2 and anti-mouse MSH6 antibodies. Antibodies that recognize endogenous MSH6 were detected as a control for loading, as the level of MSH6 is unaffected by MLH1 status in mouse and human cells. Representative extracts of cells transfected with empty vector (lanes 7, 8), vector containing the wild-type hMLH1 cDNA (WT-1, -2, -4; lanes 1-6), or containing the MLH1 cDNA with the MLH1-E578G mutation (lanes 9, 10) are shown. MC5 is non-transfected MEF cell line established from MMR-proficient embryos. The anti-hMLH1 antibody used doesn't detect the presence of mouse MLH1 protein in extracts from wild type MEFs.

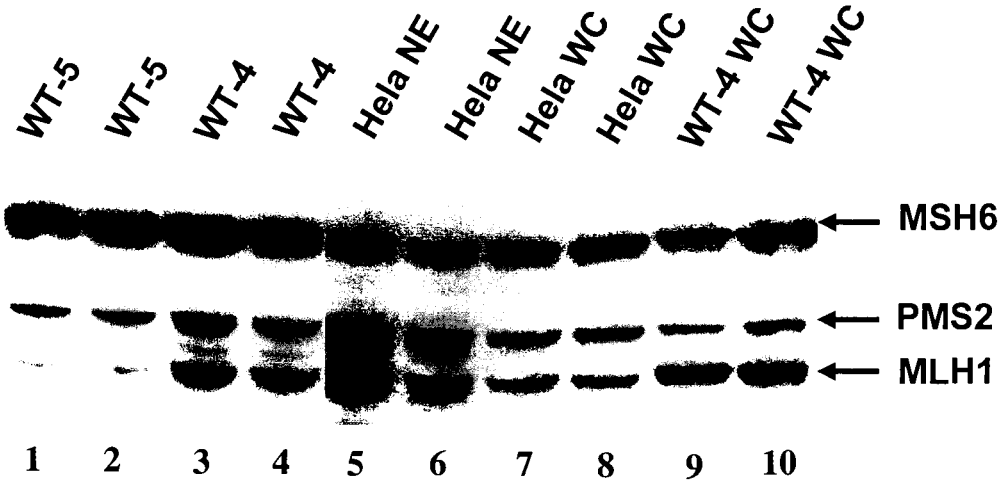

FIGURE 9. MMR PROTEIN ABUNDANCE IN HELA NUCLEAR AND MEF CYTOPLASMIC EXTRACTS

MMR protein abundance in cytoplasmic extracts of MLH1-expressing MEF lines (WT-5, WT-4; 30 μg each lanes 1-4) was compared to HeLa nuclear extracts (20 μg, lanes 5, 6) by western blot analysis. The protein abundance in whole cell lysate (30 μg lanes 7-10) in HeLa and WT-4 cells also was compared.

To determine the relative concentration of MLH1 in the different extracts, purified MutLα (kindly provided by R.M. Liskay Oregon Health Science University) (Tomer *et al,* 2002) was used to generate a standard curve for MLH1 chemiluminescence signals. Signal intensities were compared to signals from cytoplasmic extracts of WT-1 and WT-2 MEF lines, and from nuclear extracts of HeLa cells (Figure 10). The concentration of MLH1 in WT-1 extracts was determined to be 170 fmoles /100 μg extracts protein, whereas the concentration in nuclear extract was 620 fmoles /100 μg extracts protein. A similar approach used previously reported a concentration of MLH1 of 160 fmoles/ 100 μg nuclear extracts (Genschel, 2003), approximately 4 times lower than my estimate. The reason for the difference in MLH1 concentration in nuclear extracts is not known, but may reflect differences in extract preparation or methodology for measuring the concentration of purified MutLα preparations. Based on the concentration of MLH1 determined for WT-1 extracts and the relative signal intensities for MLH1 measured in the analysis presented above (Figures 8 and 9), I estimated the MLH1 protein concentration in the various cytoplasmic extracts used (Figure 11). Apparent MLH1 concentrations in extracts of wild-type expressing cells ranged from 7-170 fmoles/ 100 μg extracts protein and generally were greater than the MLH1-E578G concentrations in extracts of two representative MEF lines. MLH1 concentration in HeLa nuclear extract was 3-4 times higher than in the transfected MEF lines.

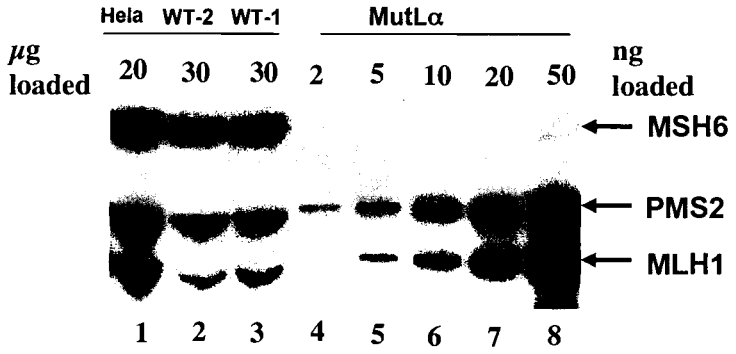

FIGURE 10. MUTLα CONCENTRATIONS IN DIFFERENT EXTRACTS

Chemiluminescence signal intensities for MLH1 and PMS2 in reference amounts of purified MutLα (lanes 4-8) and the indicated amounts of nuclear or cytoplasmic extracts (lanes 1-3) were compared following western blot analysis. Using same extracts, similar results were obtained from 2 other independent blots.

3.4.1 MMR in extracts of cells expressing different levels of MLH1

Two different methods were used to determine the relationship between repair activity and MLH1 concentration in the cytoplasmic extracts. First, I compared the repair efficiencies of cytoplasmic extracts with different levels of MLH1; for example, WT-4 extracts have a lower MLH1 concentration than WT-1 extracts. To determine if repair efficiency differs in different transfectants that express different levels of MLH1, an alternative approach used (in section 3.4.2 MMR in diluted cytoplasmic extracts) was to manipulate the level of MLH1 in extracts, and then measure repair activity. Using cytoplasmic extracts of several different cell lines expressing different levels of MLH1, MMR reactions were run simultaneously in parallel using the C-loop mismatched substrate. Controls included extract of vector-transfected cells and reactions with no added extract. One representative experiment using 3 different extracts is presented (Figure 12A). Repair efficiencies (calculated as the percent yield of repaired product relative to input amount of substrate) of different extracts did vary. As expected, vector and no extract controls yielded no repaired products. To determine the MLH1 concentration dependence for repair, measured repair efficiencies from multiple experiments were plotted as a function of apparent MLH1 concentrations (Figure 11), and analyzed by linear regression (Figure 12B), yielding an r^2 value of 0.89 for the best-fit line. Similar experiment conducted using the CT-loop mismatched substrate (Figure 13) was analyzed in the same manner, yielding an r^2 of 0.76 for

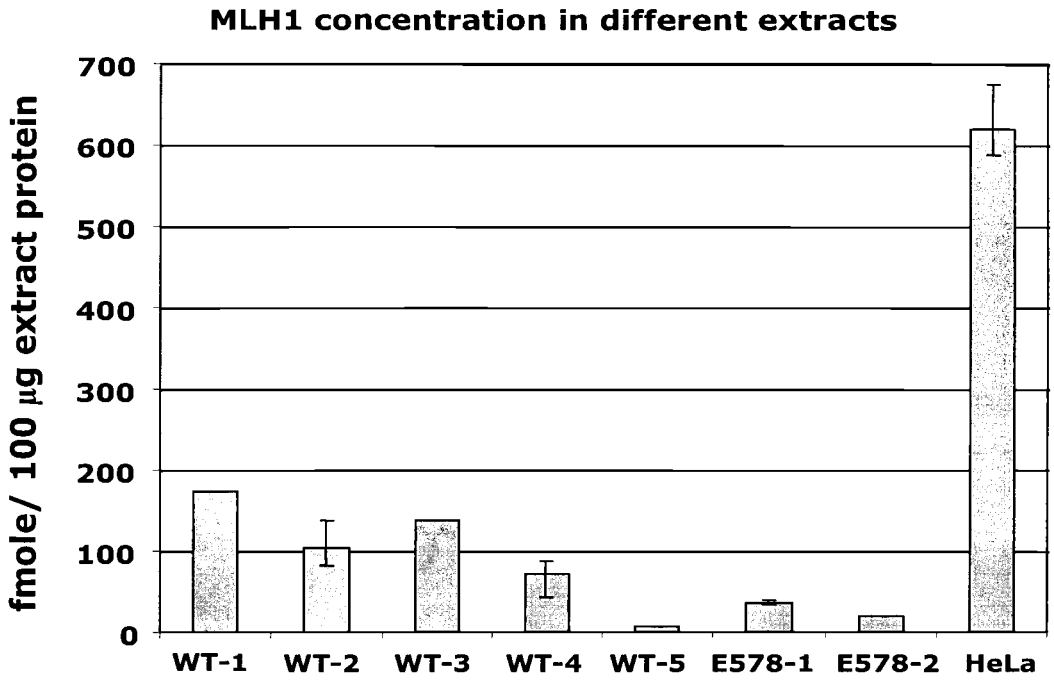

FIGURE 11. MLH1 CONCENTRATION IN CYTOPLASMIC AND NUCLEAR EXTRACTS

Relative chemiluminescence signals for MLH1 in different extracts were compared to signals for cytoplasmic extracts of WT-1 cells and used to estimate MLH1 concentration. Relative signals were averaged from at least three independent western blots.

the best-fit line. While repair efficiencies measured with CT-loop mismatch were higher (up to approximately 70% repair) than with the C-loop mismatch (up to approximately 50% repair), generally the trends were similar. With both substrates, repair appeared to increase linearly with increasing concentration of MLH1 in the extracts.

3.4.2 MMR in diluted cytoplasmic extracts

To confirm that MMR in cytoplasmic extracts of transfected MEFs was linearly dependent upon MLH1 concentration, I manipulated the concentration of MLH1 in cytoplasmic extracts by dilution and measured repair in the diluted extracts. To maintain similar concentrations for other proteins involved in MMR, the dilutant used was cytoplasmic extract of vector-transfected MEFs. The dilutant vector-transfected extract was confirmed to contain all necessary MMR factors besides MutLα. In control reactions, purified MutLα (Tomer *et al,* 2002) was sufficient to restore MMR activity to the vector-transfected extract (data not shown). In addition, western blot analysis confirmed that MSH6 levels in diluted extracts and undiluted extracts were similar (Figure 14 and data not shown). Repair activities with different diluted extracts were tested using a C-loop mismatched substrate (Figure 15 and 16) and analyzed as described in the previous section (Figure 12 and 13). Repair in diluted WT-1 cytoplasmic extracts decreased with increasing dilution, from a maximum of 25% (undiluted extract) to below background levels with the 1:8 dilution. Similar results were obtained using a

A

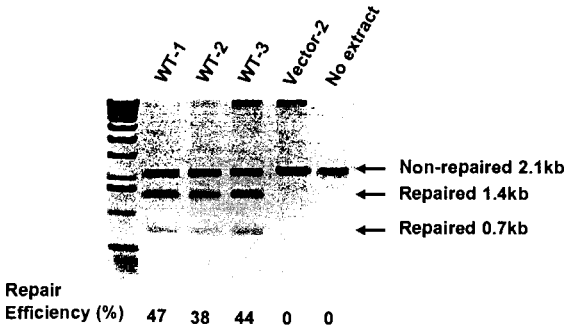

B

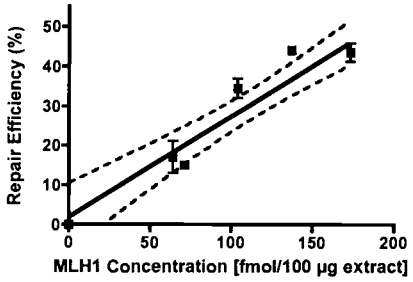

FIGURE 12. REPAIR OF C-LOOP SUBSTRATE BY DIFFERENT WILD-TYPE MLH1 EXPRESSING CYTOPLASMIC EXTRACTS

(A) Extracts of WT-1, WT-2 and WT-3 were obtained from different stable transfectants and used in *in vitro* repair reactions. Vector-transfected extract and no extract reactions were included as negative controls. With the C-loop mismatched substrate, repair was screened by Fsp-1 restriction digestion. Arrows indicate the nonrepaired and repaired products. (B) Results of repair reactions with cytoplasmic extracts of different MEF lines were plotted as a function of MLH1 concentration, and analyzed using a linear regression model. Plotted for each extracts are averages (13-47%) of at least 3 individual experiments. Dashed lines indicate 95% CI.

A

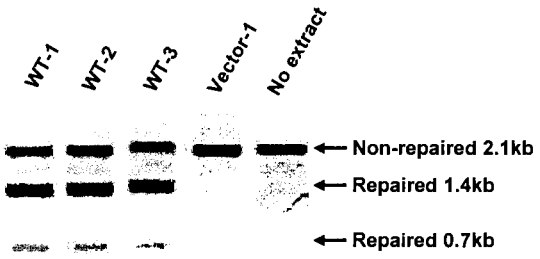

Repair Efficiency(%)	70	65	69	0	0

B

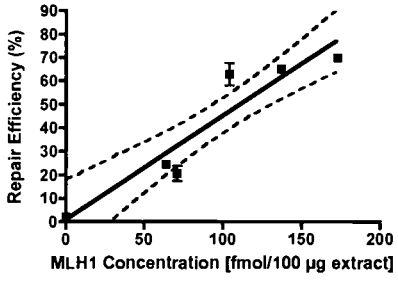

FIGURE 13. REPAIR OF CT-LOOP SUBSTRATE BY DIFFERENT WILD-TYPE MLH1 EXPRESSING CYTOPLASMIC EXTRACTS

second diluted extract (of WT-2 cells) (Figure 16). In both cases, repair efficiencies appeared linearly dependent upon MLH1 concentration, yielding r^2 values of 0.91 and 0.97 for diluted extracts of WT-1 and WT-2 cells, respectively. In neither case, did repair efficiencies plateau. These results are consistent with the analysis of repair using extracts of cells expressing different levels of MLH1 (Figures 12 and 13), together suggesting that MLH1 is limiting for *in vitro* repair using cytoplasmic extracts of transfected MEFs.

3.5 Kinetics of MMR in cytoplasmic extracts

To determine the kinetics of repair in cytoplasmic extracts, the appearance of repair products was measured at various times of incubation from 3-20 minutes, using both the C-loop and CT-loop substrates, and extracts prepared from WT-1 cells. In each experiment, reaction mixes sufficient for multiple reactions were assembled. Repair was initiated by addition of extract and transfer of reaction tubes

FIGURE 14. MMR PROTEIN LEVELS IN DILUTED CYTOPLASMIC EXTRACTS

WT-1 cytoplasmic extracts were diluted with vector-transfected cytoplasmic extract at the indicated ratios (WT-1: Vector), and analyzed by western blotting.

A

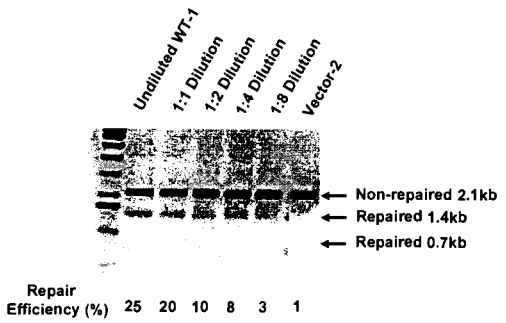

B

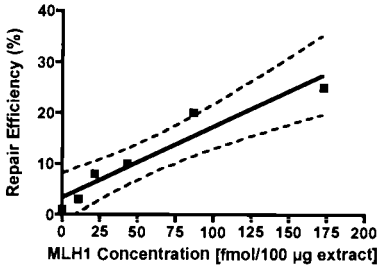

FIGURE 15. REPAIR OF C-LOOP BY DILUTED WT-1 CYTOPLASMIC EXTRACT

(A) Agarose gel analysis of in vitro MMR by diluted WT-1. WT-1 extract was diluted into vector extract and then incubated with 100 ng of C-loop substrate at 37°C for 15 minutes; the repaired product was screened with FspI restriction digestion. The arrows indicate the non-repaired 2.1 kb substrate and the repaired fragments 1.4 kb and 0.7 kb. Vector extract was used as negative control for in vitro repair. (B) Repair result in A was plotted. Results of C-loop repair by WT-1 extracts plotted, the solid line represents the best-fit linear regression curve. The MLH1 concentration was obtained by comparing the protein abundance in extracts to purified MutLα. Dash lines represent 95% CI.

A

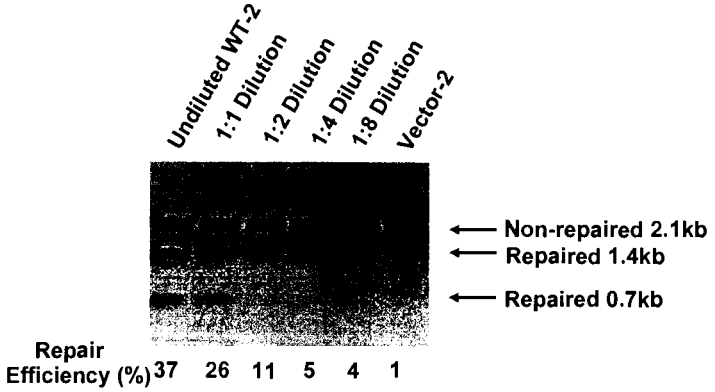

B

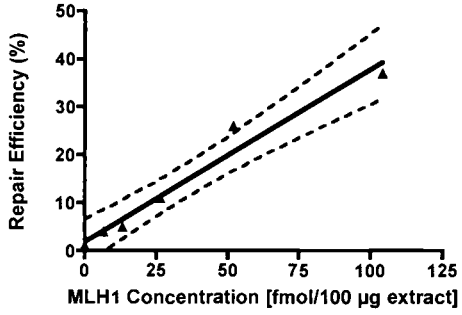

FIGURE 16. REPAIR OF C-LOOP BY DILUTED WT-2 CYTOPLASMIC EXTRACT

(A) Repeat of the dilution experiment by different wild-type MLH1 expressing cytoplasmic extract-WT-2. B. Repair result in A was plotted.

to a 37°C water bath. Repair efficiencies were determined by restriction digestion analysis on aliquots removed at different times of incubation. As shown in Figure 17, repair efficiency increased with both substrates up to approximately 10 minutes, after which there were no further significant increases. Similar results were reported previously by using HeLa cell nuclear extracts (Wang, 2002), in which repair was shown to reach a plateau by approximately 8 minutes. Thus repair in cytoplasmic extracts proceeds with similar kinetics as is seen using HeLa cell nuclear extracts.

3.6 Activity of MLH1-E578G in MMR

Analysis of *in vitro* repair of C-loop and CT-loop mismatches using cytoplasmic extracts of transfected MEF cell lines (Figures 12 and 13) indicated that repair is linearly dependent upon MLH1 concentration and that repair reaches plateau levels within approximately 10 minutes. Therefore, an evaluation of the ability of MLH1-E578G (or other variants) to function in MMR in this system should use extracts with equivalent concentrations of wild-type or mutant MLH1, and should be measured at time points prior to 10 minutes in order to compare initial rates of repair. However, cytoplasmic extracts of available cell lines expressing MLH1-E578G contained fairly low concentrations of the mutant MLH1. Even with the wild-type MLH1, the repair efficiency with such levels of MLH1 is expected to be fairly low, especially when measured at early time points.

A

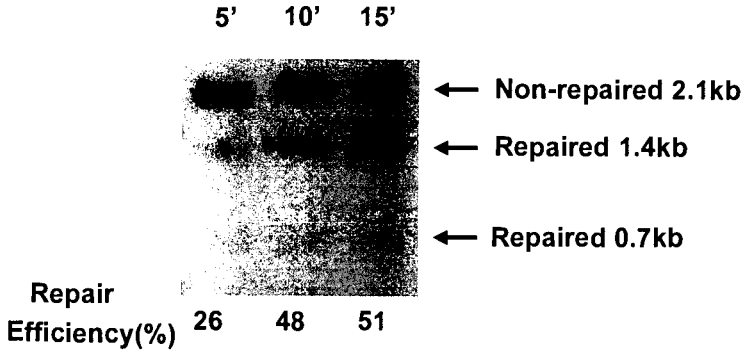
5'
10'
15'
Non-repaired 2.1kb
Repaired 1.4kb
Repaired 0.7kb
Repair
Efficiency(%)
26
48
51

B

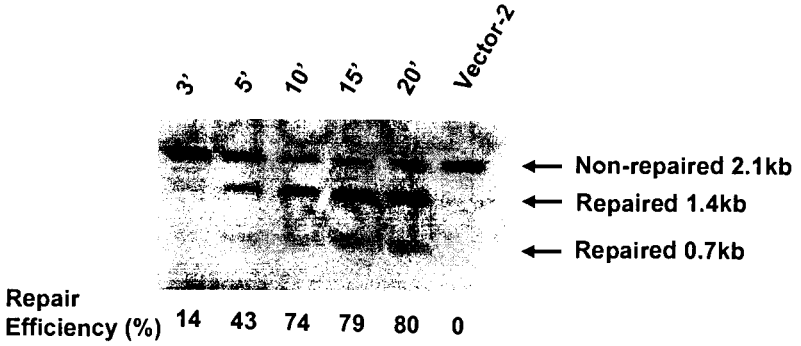
3'
5'
10'
15'
20'
Vector-2
Non-repaired 2.1kb
Repaired 1.4kb
Repaired 0.7kb
Repair
Efficiency (%)
14
43
74
79
80
0

C

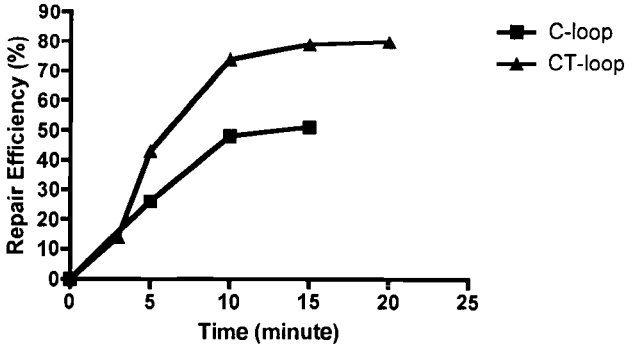
Repair Efficiency (%)
90
80
70
60
50
40
30
20
10
0
0
5
10
15
20
25
Time (minute)
C-loop
CT-loop

FIGURE 17. KINETICS OF MMR IN CYTOPLASMIC EXTRACTS

The kinetics of repair was measured with C-loop (A) by restriction digestion as in previous figures or CT-loop (B) mismatched substrates using extracts of wild-type MLH1-expressing cells. Repair efficiencies measured in (A) and (B) were plotted as a function of time (C).

In anticipation of such difficulties, I chose to compare repair efficiencies of wild-type and MLH1-E578G extracts by measuring plateau levels of repair. To account for the low concentration of MLH1-E578G, I compared the repair efficiency in MLH1-E578G containing extracts to the repair efficiency predicted for wild-type MLH1-containing extracts of similar MLH1 concentration based on a standard curve. Two standard curves were generated; one each for the C-loop and CT-loop substrate, by pooling results generated using extracts of cells expressing different levels of MLH1 (Figures 12 and 13), and using extracts diluted with vector-transfected extracts (Figures 15 and 16). The pooled results were plotted together and analyzed by linear regression to generate a best-fit line and 95% CI (Figure 18). The best-fit line for each data set was presumed to represent the level of repair to be expected for any given concentration of MLH1 within the range of concentrations examined.

Repair reactions were performed using extracts of cells expressing MLH1-E578G and analyzed by restriction digestion as described in previous sections. Using C-loop mismatched substrate, MLH1-E578G extract yielded a repair efficiency of 26% versus 15-30% repair for wild-type MLH1 control extracts and < 5% apparent repair in negative control reactions (Figure 19). When plotted versus the standard curve generated with wild-type MLH1-containing extracts and using the concentration of MLH1-E578G determined in Figure 11, repair efficiency with MLH1-E578G was within the expected range for wild-type MLH1 of the same

concentration. Similar results were obtained with CT-loop substrate (Figure 20). These results were similar to results of the repair reaction using a G/T mismatched substrate (Figure 7), in which repair in an MLH1-E578G extract was comparable to repair in a wild-type MLH1 extract. Similar results also were obtained using cytoplasmic extracts of transfected human ovarian cell lines (data not shown). Although extracts of the human cells containing comparable levels of wild-type MLH1 and MLH1-E578G were obtained (approximately 125 fmole/ 100 μg extract), these extracts lost activity very quickly upon storage, generating somewhat inconsistent results and precluding a definitive analysis.

Taken together, the results demonstrated that MLH1-E578G is capable of supporting the *in vitro* repair of several classes of mismatches. The activity of MLH1-E578G appears comparable to that of wild-type MLH1; however, these comparisons were made using plateau levels of repair, which precludes detection of modest defects in activity.

A

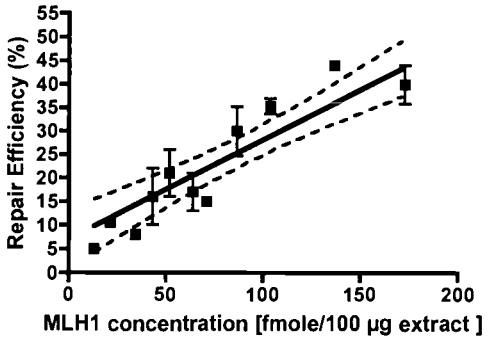

B

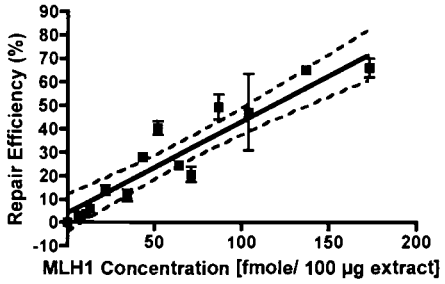

FIGURE 18. STANDARD CURVE OF C-LOOP (A) AND CT-LOOP (B) REPAIR

Standard curve were generated by pooling results generated using extracts of cells expressing different levels of MLH1 (Figures 12 and 13), and using extracts diluted with vector-transfected extracts (Figures 15 and 16).

A

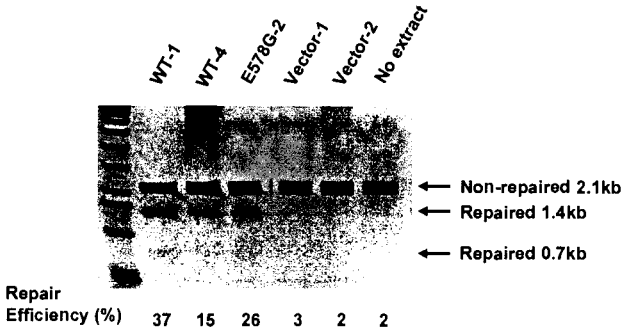

B

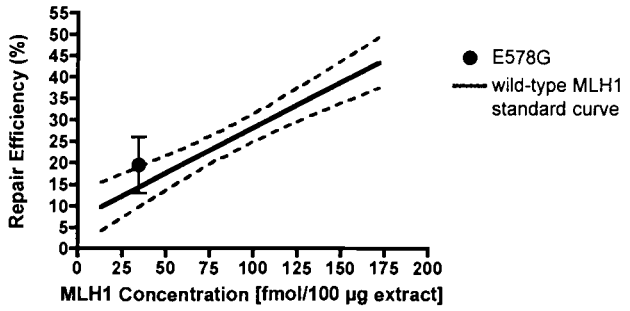

FIGURE 19. C-LOOP MMR IN MLH1-E578G CYTOPLASMIC EXTRACTS

(A) Restriction digestion of *in vitro* repair using the C-loop mismatched substrate and extract of MLH1-E578 expressing cells, and measured after 15 minutes incubation for repair. (B) The C-loop repair efficiency supported by MLH1-E578G extract was plotted versus the wild type MLH1 standard curve (Figure 18A), plotted is the standard curve (black line) with the mean of at least 2 independent MLH1-E578G repair reactions. 95% CI (dashed lines) is generated using wild-type MLH1-containing extracts.

A

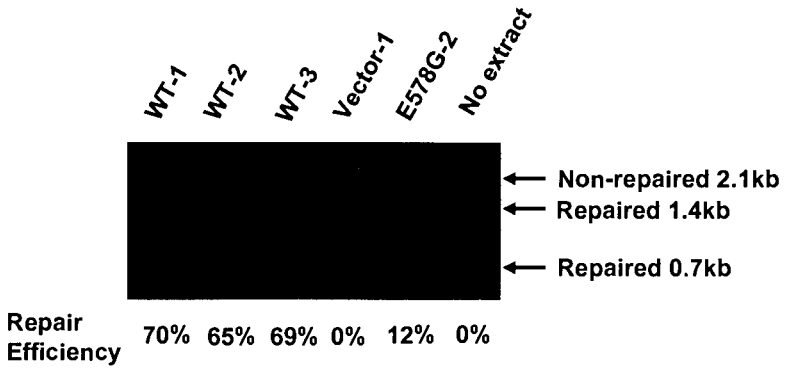

B

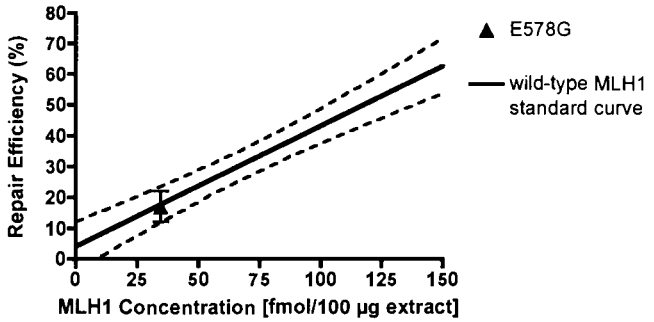

FIGURE 20 CT -LOOP MMR IN MLH1-E578G CYTOPLASMIC EXTRACTS

Analyzed similarly to Figure 19.

CHAPTER 4. DISCUSSION

This study is focused on a specific MLH1 mutation MLH1-E578G that was identified as a germline mutation in several suspected Lynch Syndrome patients. However, the impact of this mutant on disease risk and the mechanism through which this mutation might affect MMR remains unknown. I reported here an analysis of the ability of the MLH1-E578G mutant to support MLH1-dependent MMR measured *in vitro* using several different mismatched substrates and cytoplasmic extracts prepared from transfected MEF cell lines. Results presented confirm that repair-competent cytoplasmic extracts could be used for in vitro MMR assays. Repair in such extracts reached plateau levels within approximately 10 minutes, and appeared linearly dependent upon MLH1 concentration, suggesting that MutLα is a limiting factor for repair in this system. MLH1-E578G was shown to be capable of supporting MMR in vitro, using a G/T, a C-loop and a CT-loop mismatched substrate, with repair efficiencies measured at plateau levels comparable to wild-type MLH1. I conclude that extract of transfected MEFs a potentially useful system for analysis of consequences of mutations in MLH1, and that pathogenic effects of MLH1-E578G are not related to dramatically decreased repair efficiency. Other potential mechanisms for cellular deficiencies associated with MLH1-E578G should be considered.

Previously HeLa nuclear extract was characterized exclusively to develop and support current models for mechanisms of MMR (Holmes *et al,* 1990; Blackwell, 1998; Matton, 2000, Wang and Hays, 2003). However, it requires 10^9-10^{10} cells to make nuclear extract, which limits the applicability with adhesive cells. Cytoplasmic extracts were previously used for in vitro MMR assay as well (Thomas *et al,* 1991, Tomer *et al,* 2002), but this system is not characterized as thoroughly as HeLa nuclear extract. Transfection of MLH1-/- MEFs established a genetic model for analysis of phenotypic consequences of MLH1 mutations (Buermeyer, 1999; Mohd *et al,* 2005). One goal of this thesis was to determine usefulness of cytoplasmic extract of transfected MEFs as a counter-part for genetic studies with the purpose of investigating biochemical mechanisms of deficiencies associated with MLH1 mutations.

As originally described (Thomas *et al,* 1991), repair in cytoplasmic extracts was scored using a blue/white plaque assay after transformation of *E. Coli* with M13-based plasmid substrates. This approach is technically challenging, and somewhat limited in range of substrates that could be tested. Subsequent studies demonstrate that repair could be scored by analysis of sensitivity to restriction digestion (O'Regan *et al,* 1996, Tomer *et al,* 2002) as described for reactions with HeLa nuclear cell nuclear extracts, and that repair was MutLα-dependent (Tomer *et al,* 2002). This wor characterized further repair reactions using cytoplasmic extracts, and demonstrated that repair efficiency can be robust (up to 70% with CT-

loop substrate) and that appearance of repair product proceeds with kinetics comparable to that reported for HeLa (Wang 2002). Although an extensive side-by-side comparison with HeLa nuclear extract was not performed, this study suggests that repair efficiencies are comparable and likely utilize the same mechanisms.

One interesting new finding in this study is the determination that MLH1 and PMS2 (MutLα) levels are significantly lower in cytoplasmic extracts than in HeLa. Further analysis indicated that repair is linearly dependent upon MLH1 concentration, suggesting that MLH1 (and by extension MutLα) is limiting for repair. Measurement of initial rates of repair with limiting amounts of MutLα should allow quantitative comparison of the repair activities for wild-type and mutant MLH1.

The biochemical analysis of MLH1-E578G was prompted by interest in this mutation as potentially pathogenic, and by cell culture studies in the Buermeyer laboratory that suggested MLH1-E578G was selectively defective in repair of base-base mismatches while proficient for repair of dinucleotide loops. This study showed that extracts of cells expressing MLH1-E578G were proficient for repair of a G/T, a C-loop and a CT-loop mismatch, suggesting that the glycine substitution does not dramatically interfere with MLH1 function. As repair was measured at 15 minutes, I cannot rule out a modest defect in activity associated with the MLH1-E578G mutation. However, there did not appear to be a specific defect in the repair of base-base mismatch versus the loop-mismatched substrates. Also, the present

data cannot rule out the possibility of a defect in repair of other specific mismatches or mismatches in other sequence contexts.

Apparently, proficient repair of base-base mismatches by MLH1-E578G leaves the cellular phenotype of an increased rate of base-substitution in MLH1-E578G-expressing cells unexplained. However, more recent analysis by others in Buermeyer laboratory has suggested that the available MLH1-E578G-expressing cell lines actually contain a mixed population of non-expressing and expressing cells (Buermeyer, unpublished). The appearance of non-expressing cells within the population analyzed seems to be an inherent property of the cell line in which expression of the recombinant MLH1-E578G is lost within a subset of cells in the population, and could explain both an apparent increase in mutation rate, and variability in MLH1-E578G expression in culture, and concentration in extracts over time. Proficient repair of loop-mismatches by MLH1-E578G is consistent with a lack of MSI detected in cancers with this mutation. However, the repair proficiency observed does not help explain an apparent increased disease risk associated with MLH1-E578G. More recent work in Buermeyer laboratory (Mohd, Palama and Buermeyer, unpublished) has confirmed that MLH1-E578G can interact stably with PMS2 to form the MutLα heterodimer. However, MLH1-E578G did display a modest reduction in protein stability in cells. Reduced stability for MLH1 has been reported for other pathogenic mutations (e.g. MLH1-K616 del) (Raevaara 2005), and could contribute to an increased risk of disease associated

with MLH1-E578G. Consistent with this hypothesis, is a similarly reduced stability associated with a second mutation, MLH1-K618A that also was identified in MSI-negative cancers.

BIBLIOGRAPHY

Allen DJ, Makhov A, Grilley M, Taylor J, Thresher R, et *al.* 1997. MutS mediates heteroduplex loop formation by a translocation mechanism. *EMBO J.* 16:4467-76

Ana Sánchez de Abajo *et al* 2005 Low prevalence of germline hMSH6 mutations in colorectal cancer families from Spain. *World J Gastroenterol* ISSN 1007-9327 CN 14-1219/R October 7;11(37):5770-5776

Au KG, Welsh K, Modrich P. 1992. Initiation of methyl-directed mismatch repair. *J. Biol. Chem.* 267:12142-48

Ban C, Yang W. 1998. Crystal structure and ATPase activity of MutL: implications for DNA repair and mutagenesis. *Cell* 95:541-52

Bellacosa A. 2001. Functional interactions and signaling properties of mammalian DNA mismatch repair proteins. *Cell Death Differ.* 8:1076–92

Bocker T, Barusevicius A, Snowden T, Rasio D, Guerrette S, et al. 1999. hMSH5: a human MutS homologue that forms a novel heterodimer with hMSH4 and is expressed during spermatogenesis. *Cancer Res.* 59:816-22

Blackwell L, Bjornson K Modrich P. 1998 DNA-dependent activation of the hMutSα ATPase. *J. Biol. Chem.* 273: 32049-32054

Bowers J, Tran PT, Joshi A, Liskay RM, Alani E. 2001. MSH-MLH complexes formed at a DNA mismatch are disrupted by the PCNA sliding clamp. *J. Mol. Biol.* 306:957–968

Brian D. 2000. DNA mismatch repair and genetic instability. *Annu Rev. Genet.* 34:359-99

Buermeyer AB, Deschenes SM, Baker SM, Liskay RM. 1999. Mammalian DNA mismatch repair. *Annu. Rev. Genet* 33:533-564

Buermeyer AB. 1999. The human MLH1 cDNA complements DNA mismatch repair defects in MLH1-deficient mouse embryonic fibroblasts. *Cancer Res.* 59: 538-541

Claij N. 2002. Methylation tolerance in MMR deficient cells with low MSH2 protein level. *Oncogene* 21:2873-79

Fishel R. 2001. The selection for mismatch repair defects in hereditary nonpolyposis colorectal cancer: revising the mutator hypothesis. *Cancer Res.* 61:7369-74

Galio L, Bourquet C, Brooks P. 1999. ATP hydrolysis-dependent formation of a dymamic ternary nucleoprotein complex with MutS and MutL. *Nucleic Acids Res.* 27:2325-31

Genschel, J., Bazemore, L. R., and Modrich, P. 2002 Human Exonuclease I is required for 5' and 3' mismatch repair *J. Biol. Chem.* 277, 13302–1331

Genschel J. Modrich P. 2003. Mechanism of 5'-directed excision in human mismatch repair. *Molecular Cell.* 12:1077-1086

Gradia S, Acharya S, Fishel R. 1997. The human mismatch recognition complex hMSH2–hMSH6 functions as a novel molecular switch. *Cell* 91:995–100

Gradia S, Subramanian D, Acharya S, Malchov A, Griffith J, Fishel R. 1999. hMSH2–hMSH6 forms a hydrolysis-independent sliding clamp on mismatched DNA. *Mol. Cell* 3:255–61

Grilley M, Welsh KM, Su S-S, Modrich P. 1989. Isolation and characerization of the *Escherichia coli mutL* gene product. *J. Biol. Chem.* 264:1000-4

Guerrette S, Acharya S, Fishel R. 1999 The interaction of human MutL homologue in hereditary nonpolyposis colon cancer. *J. Biol.Chem.* 274: 6336-41

Gupta RD, Kolodner RD, 2000. Novel dominant mutations in *Saccharomyces cerevisiae MSH6*, *Nat. Genet.* 24:53-56

Hall MC, Matson SW. 1999. The *Escherichia coli* MutL protein physically interacts with MutH and stimulates the MutH-associated endonuclease activity. *J. Biol. Chem.* 274:1306-12

Hall, M.C., Shcherbakova, P.V., Borchers, C., Dial, M., Tomer, K.B., and Kunkel, T.A. 2003 DNA binding by Saccharomyces cerevisiae Mlh1-Pms1: Implications for DNA mismatch repair. *Nucleic Acids Research* 31, 2025-2034.

Harfe BD, Jinks-Robertson S. 2000. DNA mismatch repair and genetic instability, *Annu. Rev. Genet* 34: 359-399

Her C, Vo AT, Wu X. 2002. Evidence for a direct association of hMRE11 with the human mismatch repair protein hMLH1. *DNA Repair* (Amst) 1: 719–729

Holmes J, Clark Jr, S, and Modrich P (1990) Strand-specific mismatch correction in nuclear extracts of human and Drosophila melanogaster cell lines. *Proc Natl Acad Sci*; 87(15): 5837–5841.

Junop MS, Obmolova G, Rausch K, Hsieh P, Yang W. 2001. Composite active site of an ABC ATPase: MutS uses ATP to verify mismatch recognition and authorize DNA repair. *Mol. Cell* 7: 1–12

Lahue RS, Au KG, Modrich P. 1989. *Science* 245:160-164

Lin Yi-Ling *et al* 1998 The Evolutionarily Conserved Zinc Finger Motif in the Largest Subunit of Human Replication Protein A Is Required for DNA Replication and Mismatch Repair but Not for Nucleotide Excision Repair *J. Biol. Chem* 273:1453-1461

Liu T, Tannergård P, Hackman P, Rubio C, Kressner U, Lindmark G, Hellgren D, Lambert B and Lindblom A 1999, Missense mutations in hMLH1 associated with colorectal cancer *Human Genetics* 105:437-441

Maculloch SD, Gu L, Li GM. 2003.*J. Biol. Chem.* 278:3891-96

Marsischky GT. Filosi N, Kane MF, Kolodner R, 1996. Redundancy of saccharomyces cerevisiae MSH3 and MSH6 in MSH2-dependent mismatch repair. *Genes Dev.* 10:407-420

Matton N, Simonetti J, and Williams K 2000. Identification of Mismatch Repair Protein Complexes in HeLa Nuclear Extracts and Their Interaction with Heteroduplex DNA *J. Biol. Chem.*, Vol. 275, Issue 23, 17808-17813

Modrich P. 1991. Mechanisms and biological effects of mismatch repair. *Annu.Rev. Genet.* 25:229–53

Modrich P, Lahue R. 1996. Mismatch repair in replication fidelity, genetic recombination, and cancer biology, *Annu. Rev. Biochem.* 65:101-33

Modrich P. 1997. Strand-specific mismatch repair in mammalian cells. *J. Biol. Chem.* 272:24727-30

Mohd A, Palama B , Nelson S, Tomer G, Nguyen M, Huo X, Buermeyer A 2005 Truncation of the C-terminus of human MLH1 blocks intracellular stabilization of PMS2 and disrupts DNA mismatch repair. *DNA repair*. 2005 Dec 7

Myung K, Chen C, Kolodner RD. 2001. Multiple pathways cooperate in the suppression of genome instability in Saccharomyces cerevisiae. *Nature* 411:107376

O'Regan E, Branch P, Macpherson P, and Karran P. 1996 hMSH2-independent DNA Mismatch Recognition by Human Proteins *J. Biol. Chem.*271: 1789-1796 ;

Päivi Peltomäk 2001 Deficient DNA mismatch repair: a common etiologic factor for colon cancer *Human Molecular Genetics*, Vol. 10, No. 7 735-740

Prolla TA, *et al.* 1998. Tumour susceptibility and spontaneous mutation in mice deficient in Mlh1, Pms1 and Pms2 DMA mismatch repair. *Nature Genet.* 18: 276_279

Raevaara TE, et al. 2005. Functional Significance and Clinical Phenotype of Nontruncating Mismatch Repair Variants of MLH1. *Gastroenterology* 129:537–549

Sambrook and Russell 2001 Molecular Cloning: a Laboratory Manual Third Edition cold spring harbor laboratory press 1.65

Schofield MJ, Nayak S, Scott TH, Du C, Hsieh P. 2001. Interaction of *Escherichia coli* MutS and MutL at a DNA mismatch. *J. Biol. Chem.* 276: 28291–99

Schofield MJ, Hsieh P. 2003. DNA mismatch repair: molecular mechanisms and biological function, *Annu. Rev. Microbiol.* 57: 579-608

Shcherbakova PV, Kunkel TA. 1999. Mutator Phenotypes Conferred by *MLH1* Overexpression and by Heterozygosity for *mlh1* Mutations. *Molecular and Cellular Biology*, 19: 3177-83

Thomas DC, Roberts JD and Kunkel TA (1991) Heteroduplex repair in extracts of human HeLa cells *J. Biol. Chem.* 266: 3744-3751

Thomas, D.C., Umar, A., and Kunkel, T.A. (1995) *Methods Companion Methods Enzymol.* 7, 187-197

Tomer G, Buermeyer AB, Nguyen MM, Liskay RM. 2002. Contribution of Human Mlh1 and Pms2 ATPase Activities to DNA Mismatch Repair. *J. Biol. Chem.* 277: 21801-9

Umar A. Buermeyer AB, Simon JA, Thomas DC, Clark AB, Liskay RM, Kunkel TA. 1996. Requirement for PCNA in DNA mismatch repair at a step preceding DNA resynthesis. *Cell.* 87:65-73

Wang H, Hays JB. 2001. Simple and rapid preparation of gapped plasmid DNA for incorporation of oligomers containing specific DNA lesions. *Mol Biotechnol* 19:133-140

Wang, H., and Hays, J. B. 2002 Mismatch Repair in Human Nuclear *Extracts J. Biol. Chem.* 277, 26136-26142

Wang H, Hays JB. 2003. Mismatch repair in human nuclear extracts. *J. Biol. Chem.* 278:28686-693

Wang H, Hays JB. 2004. Signaling from DNA mispairs to mismatch-repair excision sites despite intervening blockades. *EMBO Journal* 23:2126-2133.

Wu TH, Marinus MG. 1999. Deletion mutation analysis of the mutS gene in *Escherichia coli*. *J. Biol. Chem.* 274:5948-52

Yuan. F *et al*, 2004. Evidence for involvement of HMGB1 protein in human DNA mismatch repair. *J. Biol. Chem.* 279(20): 20935 - 20940.